## SUPPLEMENTARY MATERIALS AND METHODS

### Patient biopsies and fibroblast culture

4 mm skin biopsies from AEC patients were obtained after receiving IRB approval and written informed consent from research participants or their parents. Small pieces of the tissue were briefly allowed to adhere to the bottom of dry wells before being cultured in DMEM-HG (Invitrogen, Carlsbad, CA) supplemented with 20% Earle's Salts Medium 199 (Invitrogen) and 10% FBS (Invitrogen), with 1% GlutaMAX (Invitrogen), 1% penicillin/streptomycin (Invitrogen), 100uM β-mercaptoethanol (Sigma-Aldrich, St. Louis, MO), and 10ng/mL bFGF (PeproTech, Rocky Hill, NJ). Fibroblast outgrowth was observed between 2 and 14 days after plating. Fibroblasts were serially passaged using 0.05% trypin-EDTA (Invitrogen) and maintained in human fibroblast growth medium: KO-DMEM (Invitrogen) supplemented with 2% FBS, 1% GlutaMAX, 1% non-essential amino acids (Invitrogen), 1% ITS-X (Invitrogen), 100uM β-mercaptoethanol, and 10ng/mL bFGF. Tissue explants and fibroblasts were cultured in 5% CO2 at 37$^{o}$C.

### Generation of iPSC

Genomic DNA was isolated from all patient fibroblast cultures using standard procedures. A DNA sequence analysis (performed by the DNA Sequencing Core, UC Denver) of the *TP63* gene identified mutations in exons 13 or 14 in all patient samples, which was consistent with the diagnosis of AEC (McGrath et al., 2001). The following primer sets were used to amplify exon 13 (forward primer: 5'-CTTATCTCGCCAATGCAGTTG, reverse primer: 5'-AACTACAAGGCGGTTGTCATC) and exon 14 (forward primer: 5'-GGGAATGATAGGATGCTGTGG, reverse primer: 5'-AAGATTAAGCAGGAGTGCTT).

The present study is based on two independent patient lines designated E3 (male) and F5 (female), which carry the following mutations: I537T in patient F5, and R598L in patient E3. AEC

fibroblasts were reprogrammed into iPSC using the CytoTune iPS Sendai Reprogramming System (Invitrogen). Several clones of iPSC were established for each patient line. iPSC were maintained in a feeder-free culture system (Ludwig et al., 2006, Xu et al., 2001). Pluripotency of iPSC was assessed by immunostaining with antibodies to NANOG, TRA-1-60, and SSEA-3 (Dimos et al., 2008). Further spontaneous in vitro differentiation assays were used to demonstrate the ability of iPSC to spontaneously differentiate into mesenchymal, endodermal and ectodermal cell types (Brivanlou et al., 2003) (data not shown). Normal chromosome counts were confirmed for all iPSC lines (by the Cytogenetics Core, UC Denver). All cultures spontaneously lost the Sendai vectors between passages 7 and 10 as confirmed by qRT-PCR using Sendai virus-specific primers (data not shown).

**Gene correction of AEC mutations in iPSC**

We utilized both TALEN technology (applied to E3 line) and CRISPR/CAS technology (applied to the F5 line) to correct *TP63*-AEC mutations in patient iPSC lines. The TALEN approach was based on a dimeric FOKI nuclease (Boch et al., 2009, Christian et al., 2010, Miller et al., 2011, Zhang et al., 2011). The two TALEN targeting components (pTAL.CMV-T7.016577 Left, and pTAL.CMV-T7.016586 Right) were obtained from Cellectis (Paris, France). The CRISPR/Cas approach utilized a Cas9 nickase and two gRNAs (Cong et al., 2013, Mali et al., 2013, Ran et al., 2013) targeting the *TP63*-AEC locus. Both genome editing approaches utilized gene targeting vectors carrying normal *TP63* sequence as well as silent mutations to identify recombinant (gene-corrected) alleles. These silent mutations were also designed to suppress further DNA binding of the designer nucleases and thus secondary cleavage of gene-corrected *TP63* gene loci (Supplementary Figure S1).

**Differentiation of iPSC into keratinocytes (iPSC-K)**

iPSC were differentiated into keratinocytes through treatment with retinoic acid (RA) (Sigma-Aldrich) and bone morphogenetic protein 4 (BMP4) (R&D Systems, Minneapolis, MN) essentially as described (Guenou et al., 2009, Metallo et al., 2008). Starting at around day 45 after initiation of differentiation, we started to perform immunofluorescence analysis with antibodies against TP63 and KRT14 at each passage. Cells were used for expression studies when the population of double-positive $TP63^{+}/KRT14^{+}$ cells exceeded 90%.

**RNAseq analysis and qRT-PCR verification**

RNA from iPSC-K cultured under low calcium conditions was isolated using RNeasy Plus Mini Kits (Qiagen, Valencia, CA) [samples F5, F5GC, E3, E3GC]. The libraries were generated and sequenced (150bp paired end reads) using Illumina 4000 HT sequencer by the Microarray and Genomics Core at the University of Colorado-Anschutz Medical Campus. The raw sequencing reads were converted to FASTQ files and the quality of the reads was determined using FastQC tool. Low quality reads and Illumina sequencing adapters from the 3' end of the reads were removed using the cutadapt tool. High quality reads were then mapped using STAR (version 2.5.1a) onto the human genome hg19 (NCBI 37). The *TP63* mutations in the patient samples were confirmed by visualizing the reads that mapped to exons 13 and 14 of *TP63* using the integrated genome viewer (IGV). Gene counts were determined using HTSeq tool. Normalization of reads, differential expression, and principal component analyses (PCA) were carried out using DESeq2 bioconductor package within the R statistical programming environment. Pathway identification and gene set enrichment analysis (GSEA) were performed on the genes that were significantly (adjusted p-value 0.1) deregulated (up- and downregulated) in patient samples when compared to gene corrected samples. The RNAseq data are publicly available under accession number GSE109185.

Differential gene expression was validated using qRT-PCR analysis. For this purpose, RNA was isolated using an RNeasy Plus Mini Kit (Qiagen) and cDNA was generated using a High-Capacity cDNA Reverse Transcription Kit. The LightCycler 480 SYBR Green I Master Mix (Roche, Pleasanton, CA) was used for amplification of cDNA with the CFX96 Touch System (Bio-Rad, Hercules, CA). Gene-specific TaqMan probes were obtained from ThermoFisher Scientific (Waltham, MA). Expression levels of all tested genes were normalized against levels of the keratinocyte marker gene basonuclin (BNC1a). Expression levels were determined with the comparative CT ($\Delta\Delta$CT) method.

**Western blotting**

Western blots were performed using total cell lysates following standard procedures.

**Dispase assay**

A standard dispase assay to assess cell-cell adhesion of iPSC-K in the presence and absence of the p38 inhibitor SB202190 (Sigma-Aldrich) was performed essentially as described (Chen et al., 2008, Hartlieb et al., 2014) The assay was repeated twice with cells from line F5 (F5, F5GC).

**Immunofluorescence microscopy**

Formalin-fixed and paraffin-embedded skin sections and methanol-fixed cell preparations were processed for immunofluorescence staining following standard procedures. Sample embedding and sectioning (paraffin) was done by the UC Denver Histology Core. The following antibodies were used: NANOG (rabbit polyclonal, 1:500, Abcam, Cambridge, MA), SSEA-3 (MC-631, rat monoclonal, 1:100, R&D Systems, Minneapolis, MN), TRA1-60 (TRA1-60, mouse monoclonal, 1:500, Chemicon, Billerica, MA), and TRA1-81 (TRA1-81, mouse monoclonal, 1:500, Chemicon), a-SMA (1A4, mouse monoclonal, 1:500, Sigma-Aldrich), AFP (rabbit polyclonal, 1:500, DAKO, Santa Clara, CA), and TUBB3 (rabbit polyclonal, 1:1000, Sigma-Aldrich); p63 (rabbit polyclonal,

1:100, Cell Signaling Technology Inc, Danvers, MA), DSC3 (U114, mouse monoclonal, 1:10, Fitzgerald Industries Intl, Acton, MA), DSG1/2 (DG3.10, mouse monoclonal, 1:10, RDI), DSG3 (5H10, mouse monoclonal, a generous gift provided by James Wahl, University of Nebraska), DSP1/2 (mouse polyclonal, 1:10, RDI, Flanders, NJ), JUP (PG5.1, mouse monoclonal, 1:100, Fitzgerald), KRT1 (guinea pig polyclonal, 1:50, a generous gift from Dennis Roop, UC Denver), and KRT14 (guinea pig polyclonal, 1:75, a gift from Dennis Roop). Secondary (Alexa Fluorochrome-labeled) antibodies were purchased from Invitrogen. Fluorescence staining was documented with a Nikon Eclipse 90I microscope equipped with a Coolsnap HQ2 and a DS-Fi1 camera. Image processing was done with the NIS Elements 3.10 imaging software (Nikon Instruments Inc, Melville, NY).

**Supplementary Figure 1. Overview of *TP63-AEC* target sites and correction strategies. (a)** Basic strategy of TALEN-mediated gene correction to eliminate an exon 14 *TP63* mutation in patient E3 iPSC. *TP63* exon sequences are shown in capital letters. The AEC point mutation is shown in red letters (underlined). Orange underlined sequence in the gene targeting vector (exchange matrix) represents silent mutations designed to prevent re-cutting of the gene-corrected AEC locus by the TALEN/FokI nuclease. The gene-corrected sequence is shown in green (underlined). RVD: repeat-variable di-residue.

**Supplementary Figure 1a: TALEN-Mediated Gene-Correction of Exon 14 Mutation**

**(b)** A dual sgRNA CRISPR/Cas9n approach was used to correct the *TP63-AEC* mutation in exon 13 of patient F5 iPSC. *TP63* exon sequences are shown in upper case letters. The AEC point mutation is shown in red (underlined). Sequences in blue represent the protospacer adjacent motif (PAM) sites. Orange underlined sequence in the gene targeting vector (exchange matrix) represents silent mutations designed to prevent re-cutting of the gene-corrected AEC locus by the CAS9n nuclease. The gene-corrected sequence is shown in green (underlined).

**Supplementary Figure 1b: CRISPR/CAS-Mediated Gene-Correction of Exon 13 Mutation**

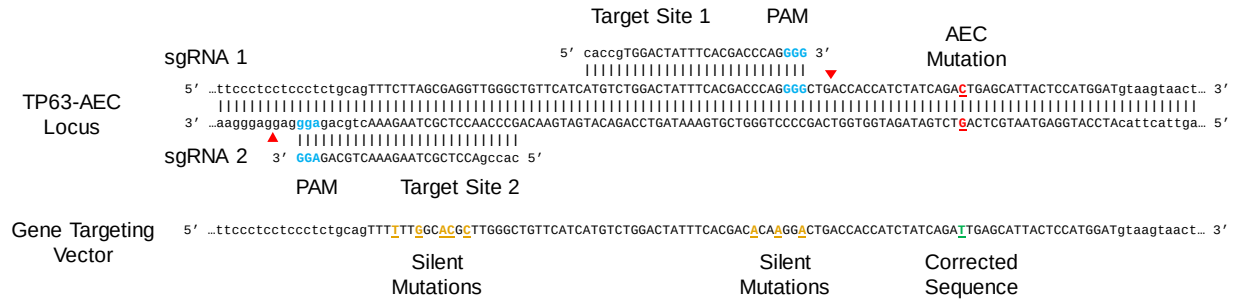


**Supplemental Figure 2. Characterization of desmosomal protein expression in AEC iPSC-K from patient E3.** Western blot analysis for the indicated proteins of a conisogenic pair of AEC and gene-corrected iPSC-K (E3 line) after exposure to high calcium conditions for 24 hours. The normalized fold changes in protein expression are indicated on the right side.

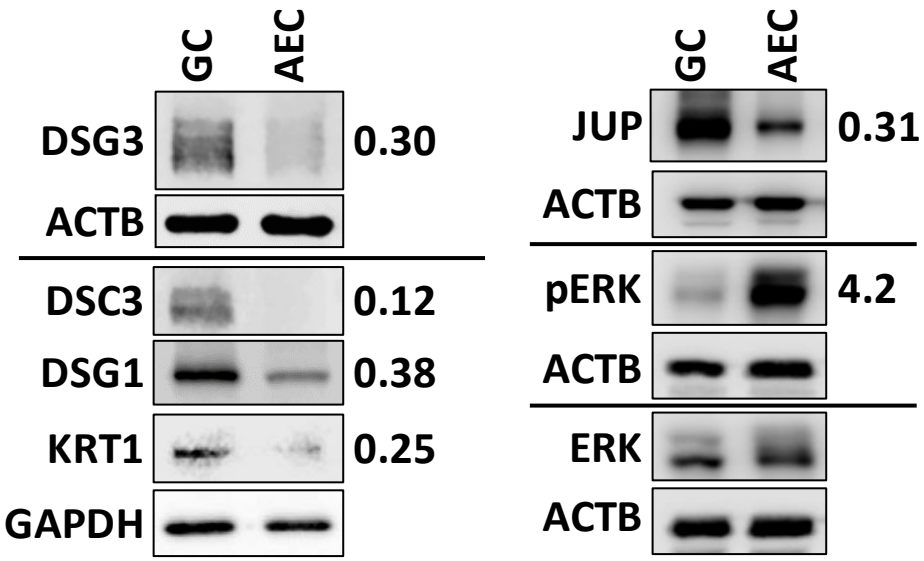
GC
AEC
DSG3
0.30
ACTB
DSC3
0.12
DSG1
0.38
KRT1
0.25
GAPDH
GC
AEC
JUP
0.31
ACTB
pERK
4.2
ACTB
ERK
ACTB

References

Boch J, Scholze H, Schornack S, Landgraf A, Hahn S, Kay S, et al. Breaking the code of DNA binding specificity of TAL-type III effectors. Science 2009;326(5959):1509-12.

Brivanlou AH, Gage FH, Jaenisch R, Jessell T, Melton D, Rossant J. Stem cells. Setting standards for human embryonic stem cells. Science 2003;300(5621):913-6.

Chen J, Den Z, Koch PJ. Loss of desmocollin 3 in mice leads to epidermal blistering. J Cell Sci 2008;121(Pt 17):2844-9.

Christian M, Cermak T, Doyle EL, Schmidt C, Zhang F, Hummel A, et al. Targeting DNA double-strand breaks with TAL effector nucleases. Genetics 2010;186(2):757-61.

Cong L, Ran FA, Cox D, Lin S, Barretto R, Habib N, et al. Multiplex genome engineering using CRISPR/Cas systems. Science 2013;339(6121):819-23.

Dimos JT, Rodolfa KT, Niakan KK, Weisenthal LM, Mitsumoto H, Chung W, et al. Induced pluripotent stem cells generated from patients with ALS can be differentiated into motor neurons. Science 2008;321(5893):1218-21.

Guenou H, Nissan X, Larcher F, Feteira J, Lemaitre G, Saidani M, et al. Human embryonic stem-cell derivatives for full reconstruction of the pluristratified epidermis: a preclinical study. Lancet 2009;374(9703):1745-53.

Hartlieb E, Rotzer V, Radeva M, Spindler V, Waschke J. Desmoglein 2 compensates for desmoglein 3 but does not control cell adhesion via regulation of p38 mitogen-activated protein kinase in keratinocytes. J Biol Chem 2014;289(24):17043-53.

Ludwig TE, Bergendahl V, Levenstein ME, Yu J, Probasco MD, Thomson JA. Feeder-independent culture of human embryonic stem cells. Nat Methods 2006;3(8):637-46.

Mali P, Aach J, Stranges PB, Esvelt KM, Moosburner M, Kosuri S, et al. CAS9 transcriptional activators for target specificity screening and paired nickases for cooperative genome engineering. Nat Biotechnol 2013;31(9):833-8.

McGrath JA, Duijf PH, Doetsch V, Irvine AD, de Waal R, Vanmolkot KR, et al. Hay-Wells syndrome is caused by heterozygous missense mutations in the SAM domain of p63. Hum Mol Genet 2001;10(3):221-9.

Metallo CM, Ji L, de Pablo JJ, Palecek SP. Retinoic acid and bone morphogenetic protein signaling synergize to efficiently direct epithelial differentiation of human embryonic stem cells. Stem Cells 2008;26(2):372-80.

Miller JC, Tan S, Qiao G, Barlow KA, Wang J, Xia DF, et al. A TALE nuclease architecture for efficient genome editing. Nat Biotechnol 2011;29(2):143-8.

Ran FA, Hsu PD, Lin CY, Gootenberg JS, Konermann S, Trevino AE, et al. Double nicking by RNA-guided CRISPR Cas9 for enhanced genome editing specificity. Cell 2013;154(6):1380-9.

Xu C, Inokuma MS, Denham J, Golds K, Kundu P, Gold JD, et al. Feeder-free growth of undifferentiated human embryonic stem cells. Nat Biotechnol 2001;19(10):971-4.

Zhang F, Cong L, Lodato S, Kosuri S, Church GM, Arlotta P. Efficient construction of sequence-specific TAL effectors for modulating mammalian transcription. Nat Biotechnol 2011;29(2):149-53.